processes

MDPI

Article

Integration of an Autothermal Outer Electrified Reformer Technology for Methanol Production from Biogas: Enhanced Syngas Quality Production and CO_2 Capture and Utilization Assessment

Loretta Salano, Marcello M. Bozzini, Simone Caspani, Giulia Bozzano * and Flavio Manenti

Dipartimento di Chimica, Materiali e Ingegneria Chimica "Giulio Natta", Politecnico di Milano, Piazza Leonardo da Vinci 32, 20133 Milano, Italy

* Correspondence: giulia.bozzano@polimi.it; Tel.: +39-0223993094

Abstract: Biogas has emerged as a valid feedstock for biomethanol production from steam reforming. This study investigates an alternative layout based on an auto-thermal electrified reforming assuming a 1 MW equivalent anaerobic digestion plant as a source for methanol synthesis. The process considers an oxy-steam combustion of biogas and direct carbon sequestration with the presence of a reverse water–gas shift reactor to convert CO_2 and H_2 produced by a solid oxide electrolyzer cell to syngas. Thermal auto-sufficiency is ensured for the reverse water–gas shift reaction through the biogas oxy-combustion, and steam production is met with the integration of heat network recovery, with an overall process total electrical demand. This work compares the proposed process of electrification with standard biogas reforming and data available from the literature. To compare the results, some key performance indicators have been introduced, showing a carbon impact of only 0.04 $kgCO_2/kgMeOH$ for the electrified process compared to 1.38 $kgCO_2/kgMeOH$ in the case of biogas reforming technology. The auto-thermal electrified design allows for the recovery of 66.32% of the carbon available in the biogas, while a similar electrified process for syngas production reported in literature reaches only 15.34%. The overall energy impact of the simulated scenarios shows 94% of the total energy demand for the auto-thermal scenario associated with the electrolyzer. Finally, the introduction of the new layout is taken into consideration based on the country's carbon intensity, proving carbon neutrality for values lower than 75 gCO_2/kWh and demonstrating the role of renewable energies in the industrial application of the process.

Keywords: biogas; steam reforming; bio methanol production; electrification; electrolyzer; hydrogen; syngas

Citation: Salano, L.; Bozzini, M.M.; Caspani, S.; Bozzano, G.; Manenti, F. Integration of an Autothermal Outer Electrified Reformer Technology for Methanol Production from Biogas: Enhanced Syngas Quality Production and CO_2 Capture and Utilization Assessment. *Processes* **2024**, *12*, 1598. https://doi.org/10.3390/pr12081598

Academic Editors: Federica Raganati and Javier Remon

Received: 14 May 2024
Revised: 12 July 2024
Accepted: 26 July 2024
Published: 30 July 2024

1. Introduction

The International Energy Agency (IEA) estimates a global expansion in the population of 21% by 2050, which brings a consequent increase in energy demand and waste production. Currently, around 80% of the energy demand is met by employing fossil fuels, which carry complications in terms of limited resources and emission of greenhouse gases [1]. Both aspects have brought international panels to push towards more sustainable energy sources [2]. International policies have been developed with the aim of reducing greenhouse gas (GHG) emissions by 85–90% by 2050, compared to 1990 [3], as well as pushing for energy supply independence, with projects like "REpower EU" [4]. The development of low-emission technologies is a crucial focus across many sectors. However, with the chemical and energy industries contributing nearly 80% of global CO_2 emissions (35 billion tons in 2019 [5]), there is a significant emphasis on advancing process technologies.

The application of renewable energy sources and alternative feedstocks for thermochemical conversion methods have emerged [6], along with studies on the role of biogas for the production of renewable hydrocarbons [7]. Biogas produced from organic waste, either from anaerobic digestion or landfills by the biological degradation of organic compounds, is a stream rich in methane and carbon dioxide. Given the number of processes directly sustained by natural gas, the potential of biogas can be exploited in various applications. Table 1 shows the dependency of biogas composition from waste sources. From 2018 to 2022, biogas production in Europe has increased by 18%, and in Italy, France, the UK, and Denmark, the production has doubled within this time span [8]. In particular, Italy is one of the EU leading countries in the sector, counting around 1600 biogas plants, with an average capacity of 752 kW [9]. Most of them are devoted to electricity and heat production through internal combustion engines. Italy. with the Budget Act of 2008, introduced an all-inclusive tariff for all biogas production plants in the 1 kW to 1 MW power production range for grid injection, with a 15-year guarantee [10]. Due to this, most of the diffused plants on Italian ground are designed to produce 1 MW of electrical power by using combined heat and power (CHP) technologies with partial heat recovery to sustain the digester energy demand and efficiencies in the range of 35–40% [11,12]. Alternative routes are available for the biogas valorization, in particular its upgrade to biomethane for injection in the natural gas grid, for use as transportation fuel either as compressed biomethane (CBM) or liquefied biomethane (LBM), and as raw material for chemicals production [13,14]. Marchese et al. introduced an energy performance for power-to-liquid applications [15], integrating carbon capture technologies within the biogas sector, while Kumar et al. brought a focus on biogas for hydrogen production, with previsions upon larger-scale production processes [16]. Zhao et al. also provided a wide review of all publications on biogas to hydrogen and syngas, showing the potential in transitioning from natural gas to biogas-based plants [17]. This approach is of great interest in the process industry field.

In the current work, the focus is on methanol production from biogas-produced syngas. The reforming of methane is currently the most widespread method for hydrogen and syngas production, covering 48% of the global demand [18,19]. The main downsides of this process are the high CO_2 emissions, in the order of 9.4–11.4 kg/kg H_2 without carbon capture and storage (CCS) systems [20], and the heat loss in the flue gases [21]. To mitigate such aspects, literature studies have emerged on the application of renewable energies to reforming technologies. Song et al. compared the performance of an electric evaporator system and a high-temperature heat pump to conventional steam methane reforming (SMR), proving their higher energetic efficiency [2]. Further studies investigated the economics of electrified methane reformers, obtaining higher production costs than standard SMR. Nonetheless, if contextualized in countries with low prices for renewable energy such as Norway and the Netherlands, the process can be considered competitive with the standard industrial route [22].

The possibility of transitioning to electrified biogas reforming plants has also emerged in recent years. Maporti et al. obtained the consumption of 1.25 kWh of renewable energy per 1 Nm^3 of hydrogen produced [23]. Moreover, another study proved an energy efficiency of 80% for a pilot plant with an estimated of only 1kWh consumption per 1 Nm^3/h of hydrogen produced [24].

Table 1. Biogas composition according to various sources.

Biogas Source	CH_4 (vol%)	CO_2 (vol%)	N_2 (vol%)	O_2 (vol%)	H_2S (ppm)	Other	Ref.
Agricultural Waste	75–45	25–55	0–25	0.01–5	<01	-	[25]
Landfill Waste	40–60	20–40	2–20	<1	40–400	C_nH_{2n+2}	[26]
Cow Manuring	55	39	5	0.9	400–1000	NH_3	[27]
Sludge	50–69	24–45	0–9	0–3	0–855	Silicon	[28]

The electrification of industrial processes has emerged as a strong route for lower impacts on emissions. In this matter, promising technologies are electrolyzers, assuming that renewable energy sources are available. Power-to-X (PTX) follows the concept of chemical production with green hydrogen as an intermediate [29]. Green hydrogen is of great interest when combined with carbon capture technologies, in particular carbon capture and utilization (CCU). CCU technologies allow the capture of CO_2 by transforming it into several valuable products (olefins, formic acid, dimethylether (DME), urea, acetic acid, methanol, and syngas) [30]. Given the availability of green hydrogen, the hydrogenation of CO_2 by reverse water–gas shift (RWGS) is one of the major approaches for the mitigation of GHG emissions (CAMERE process [31]). This process has been proposed and investigated by multiple works, proving its viability for methanol and syngas production [30,32,33].

Multiple studies have emerged on the application of biogas for methanol synthesis, going through a total upgrading to biomethane to be sent to the reforming unit [34–37]. Methanol plays a pivotal role in the achievement of net-zero targets, since it is a valuable bioenergy carrier for transportation fuel production and is a precursor of many fundamental chemical products [38]. With the provisions of national incentives and higher pressure on decarbonization, biomethanol production has also started to emerge on the market, with an estimated growth at a compound annual growth rate (CAGR) of around 25% from 2024 to 2030 [39].

In the present work, a feasibility study has been carried out for an innovative autothermal outer electrification of the biogas reforming process. The alternative layout introduces an RWGS reactor for carbon sequestration, a high-temperature electrolyzer for hydrogen and oxygen production, an oxy-steam biogas combustion chamber and an energy recovery system to ensure thermal auto-sufficiency and only electrical demand to the system. The concept of reforming is twisted in the scheme proposed, as there are still steam and biogas present as feedstock and a syngas-rich stream as a product, but no reforming reaction takes place. The work aims to prove the comparability of the alternative reforming layout to the standard process in optimal conditions for methanol production, supporting the obtained results with available literature data and a particular focus on overall energy consumption and process emissions.

2. Materials and Methods

2.1. Modeling and Design

Two case studies were considered for the validation and assessment of an alternative auto thermal outer electrification of the reforming process for methanol production. The first one, referred to as "Case A", concerns the simulation of a steam reforming of biogas, after partial removal of CO_2 by a pressure swing absorption water (PSWA) column and methanol production, while the second one, "Case B", involves the simulation of the oxy-combustion of biogas (OSC) mitigated with steam for CO_2 production with a consequent reverse water gas shift (RWGS) reactor for syngas production, a solid oxide electrolyzer cell (SOEC) for hydrogen (to be mixed with CO_2 in the RWGS) and oxygen (to sustain the OSC) production, and a methanol synthesis section. Both configurations' block schemes are reported at the top of Figure 1. The processes' mass and energy balances were performed through the software Aspen HYSYS®v11 at steady state conditions and Aspen Energy Analyzer v11®. For both simulations, the biogas feedstock is 500 Nm^3/h (607.4 kg/h), taken as the product of an anaerobic digestion plant with a size equivalent to 1MW of electrical power generation. The lower heating value is calculated on an average composition of 60 mol% of CH_4 and 40 mol% of CO_2. The inlet stream is dried and purified from impurities, such as H_2S and siloxanes, and compressed by a blower.

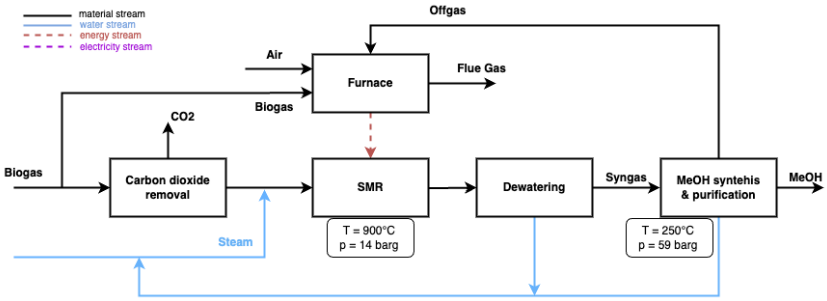

(**a**) Case A

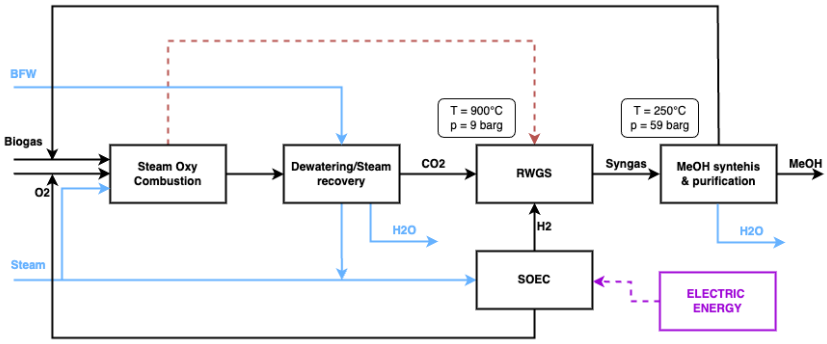

(**b**) Case B

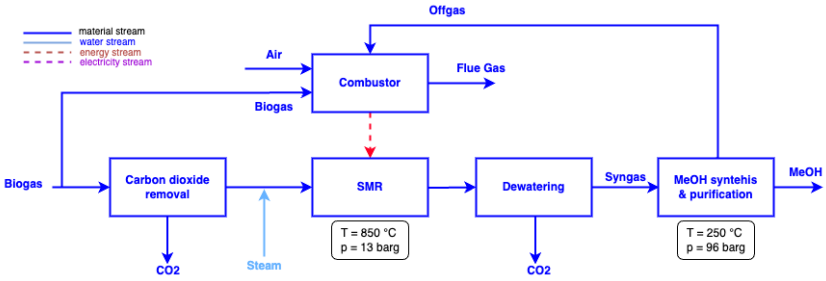

(**c**) Case C

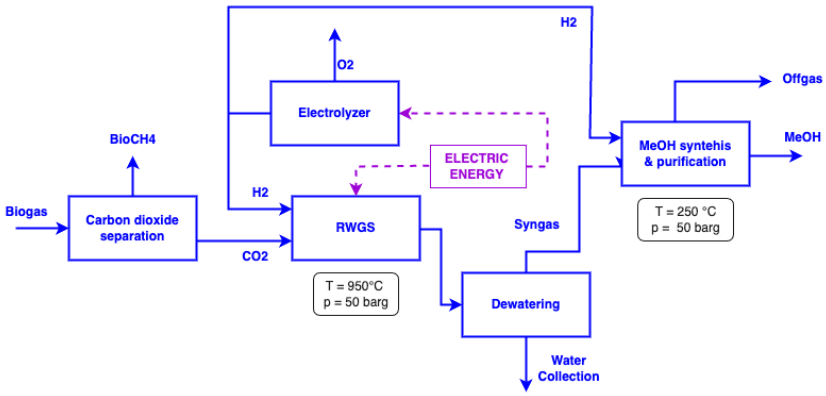

(**d**) Case D

Figure 1. Block schemes and main unit operational conditions for biogas to biomethanol production: (**a**) simulated biogas reforming of a 1 MW biogas plant; (**b**) simulated biogas autothermal outer electrified reforming of a 1 MW biogas plant; (**c**) literature reference of a biogas reforming for a 20 MW biogas plant; (**d**) literature reference for an electrification of RWGS combined with an electrolyser for a 1.7 MW biogas plant.

Further, to validate the results obtained from the simulations, two references were considered from the available literature. The first one, discussed as "Case C", refers to the work of Rinaldi et al. [35], which presents a study on the different configurations of a biogas-to-methanol process; among them, the one considered for the comparison with this work assumes the total removal of CO_2 from biogas before entering the reformer, through an amine washing unit for a 20 MW biogas plant, a steam reforming unit, and a block for methanol production, the block scheme is the third panel of Figure 1. The second study, referred to as "Case D", is related to the work of Basini et al. [40]. It compares the electrification of an RWGS reactor where the CO_2 fed to the reactor comes from the potassium carbonate washing of a stream of biogas. The stream is then sent to an electrified RWGS reactor, mixed with hydrogen from an electrolyzer. Part of the hydrogen produced is sent directly to the methanol synthesis section. This configuration considers the production of biomethane and carbon sequestration of CO_2 in the produced methanol.

2.2. Process Description: Case A

The biogas (BIOG1) is split between the furnace (BIOG2) as fuel to sustain the endothermicity of the SMR and the catalytic tubes (BIOG2) as a reactant. Before entering the reacting zone, the biogas is treated to reduce the tenor of carbon dioxide in the biogas upgrading section. The goal is to remove the right amount of CO_2 to meet the optimal condition for the subsequent methanol synthesis. The upgraded biogas (BIOG4) is mixed with steam and fed to the catalytic tubes of the reformer's furnace. The steam necessary on the tube side (STEAM) is recovered by an energy integration of the furnace's convective section and a heat exchangers recovery network. Further on, the syngas exiting the reforming unit first undergoes a water condenser, and then the dried syngas (SG1) is sent to the catalytic methanol reactor. The product is sent to two distillation column trains after recycling of the unreacted syngas (SG2) and a purge (PG1) to avoid the accumulation of methane inside the synthesis reactor. The methanol is collected at the top of the second column with a 99.85 wt% purity. A block and detailed scheme of the process are reported in Figures 1a and 2.

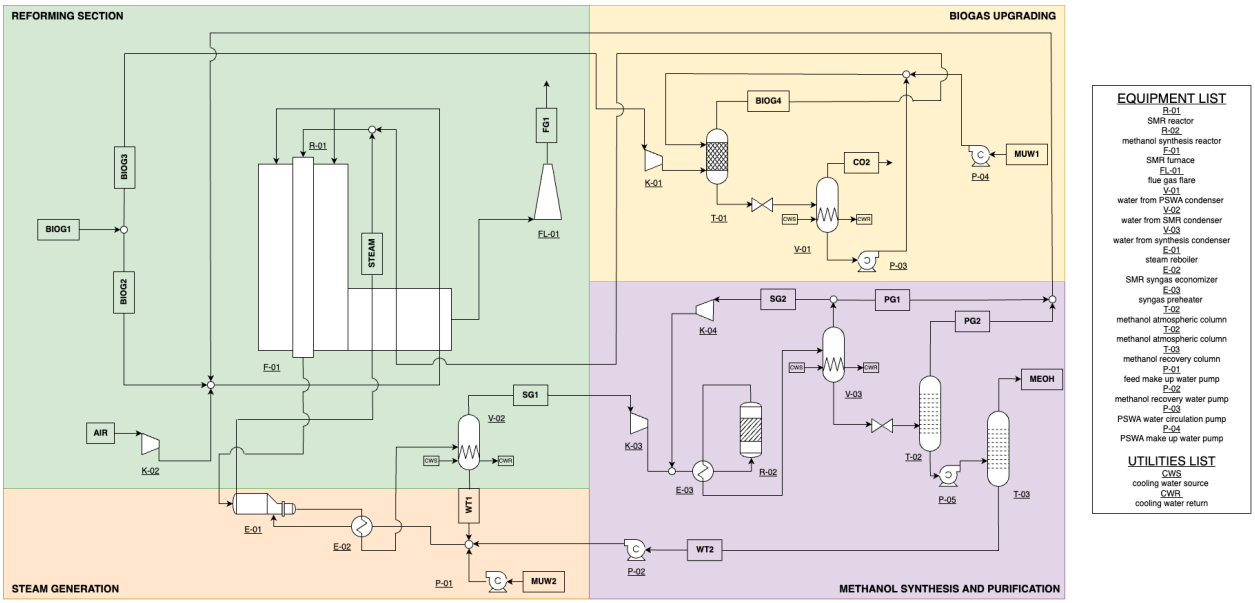

Figure 2. Process flowsheet of the SMR to methanol configuration (Case A). A simplified scheme of the heat integration is reported for better understanding. The main operational blocks are reported: biogas upgrading by a PSWA column, with recycling of water after CO_2 disengagement, the biogas reforming section with the furnace and catalytic tubes for syngas production, a steam generation section with water and heat recovery and lastly methanol synthesis reactor and purification by distillation columns.

2.2.1. Biogas Upgrading

Biogas upgrading commonly requires the full removal of CO_2 from biogas, while in this configuration, only the reforming reactor achieves a high methanol yield. Studies already available in the literature have investigated the correlation between the biogas composition and the equivalent syngas quality [41] in terms of syngas CO_2 content. In particular, optimum values have been found for methanol synthesis applications [42], measured in terms of the stoichiometric ratio (SN), defined in (1). Its theoretical value must be slightly over 2 [43,44].

$$SN = \frac{y_{H_2} - y_{CO_2}}{y_{CO} + y_{CO_2}} \quad (1)$$

Among the multiple approaches for the upgrading of biogas, the most common are: pressure swing absorption (PSA) [45], amine washing [46], water scrubbing [47], and membrane separation [48]. Santos et al. suggest the integration of a pressure swing water absorption (PSWA) column [49] for the partial removal of CO_2 for methanol synthesis, mainly due to its low energy demand and environmental impact, when compared to alternative routes. Carbon dioxide is absorbed by water at 15 bar and 20 °C in an absorption column, randomly packed in counter flow conditions and then released in a desorption tank at atmospheric pressure. The unit is designed in order to have enough hold-up to allow for the degassed water to be pumped and recycled back into the column in a continuous mode, integrated by a make-up water stream.

2.2.2. Steam Reforming

The reforming of biogas is carried out in externally heated vertical catalytic tubes employing a furnace. Operating conditions are 900 °C and 15 bars, where the reforming reactions (2) and (3) reach chemical equilibrium within the tubes [43,50].

$$CH_4 + H_2O \longleftrightarrow CO + 3H_2 \qquad \Delta H^{\circ}_{298\,K} = +206.63\ \text{kJ/mol} \quad (2)$$

$$CO + H_2O \longleftrightarrow CO_2 + H_2 \qquad \Delta H^{\circ}_{298\,K} = -41.16\ \text{kJ/mol} \quad (3)$$

The furnace sustains the endothermicity of the SMR, through the atmospheric combustion of part of the biogas in 5 mol% excess of air environment, reaching temperatures in the order of 1100 °C [51]. Steam-to-carbon ratio (SC), given by the ratio flowrate of steam $F_{steam,in}$ and methane $F_{CH_4,in}$ at the inlet of the SMR reactor (4), is adjusted to 3 to avoid coke deposition [43]. Since both units reach equilibrium at the chosen operating conditions, the furnace and catalytic reformer are implemented in the simulation as Gibbs reactors for the scope of this work. The Gibbs reactor minimizes the Gibbs free energy of the system, calculating the product mixture composition.

The steam necessary for the SMR is produced in an optimized heat recovery system, that takes advantage of the convective section of the furnace and the pre-heating of the feedstocks to improve the system efficiency and lower the flue gases temperature in the chimney [52]. Further heat recovery is met by the cooling down of the syngas produced by the reforming reacting zone, this is sent to a condenser before compression for the methanol synthesis.

$$SC = \frac{F_{steam_{in}}}{F_{CH_{4in}}} \quad (4)$$

2.3. Process Description: Case B

The alternative scheme for the electrification of biogas reforming is reported in Figure 1, while the detailed scheme is reported in Figure 3. Biogas (BIOG1) is fed with a stream of pure oxygen (OX2) and steam (STEAM1) to an oxy-steam combustion chamber where methane is consumed, producing a stream rich in CO_2 and H_2. After water condensation (WT1), the CO_2 is compressed to 10 bar and fed to an RWGS catalytic reactor, where mixing with hydrogen (HY1) allows for the hydrogenation of the CO_2 to obtain syngas. The latter

is then sent to a condenser before compression and introduction into the methanol synthesis and purification section. The hydrogen necessary for the RWGS is produced by an SOEC with simultaneous oxygen production, which is partly spent as an oxidizing agent in the OSC (OX2) and collected as a byproduct (OX3). The system is energetically integrated to allow autothermal conditions of the RWGS reactor employing the heat released by the OSC. Further, the production of steam for H_2 production and oxy-combustion mitigation is integrated into a heat recovery network. Due to this aspect, the process requires only an electrical demand, and considering the use of biogas as feedstock to produce syngas, the technology is presented as an autothermal outer electrification of a reforming process.

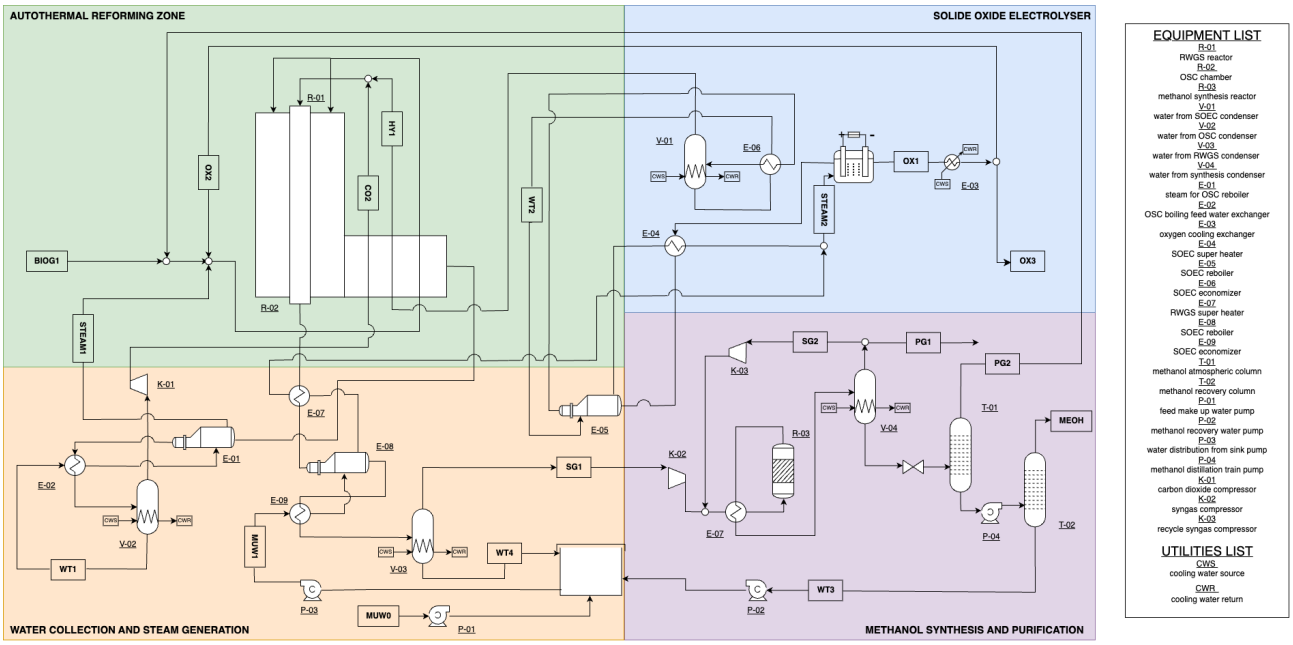

Figure 3. Simplified process flowsheet of the autothermal outer electrification of biogas reforming for methanol production. The configuration is divided into main blocks, the autothermal reforming zone is represented in green, where the OSC and RWGS are set with a similar configuration to standard SMR. Oxygen and hydrogen are provided by the SOEC, marked in the blue block, with an excess production of oxygen. The syngas produced by the RWGS is sent to the methanol synthesis and purification area (in purple). The water from the condensation steps is collected in a tank with the make-up water, to be used as a source for the necessary steam production.

2.3.1. Oxy Steam Combustion

The methane feed participates in an oxy-steam combustion (reactions (5)–(7)), which is a promising technology for reducing carbon dioxide emissions and has a low technological risk for industrialization. Oxygen is used instead of air as the combusting agent, and steam acts as the thermal diluent, together with the CO_2 present, to mitigate the high temperatures produced by the combustion. This technology has many advantages: other than its lower emission impact, it allows for a compact system, ease of operation, smaller sizing, and overall energy savings. This unit was implemented as a Gibbs reactor.

$$CH_4 + 2O_2 \rightarrow 2H_2O + CO_2 \qquad \Delta H^{\circ}_{298\,K} = -802.63\,\text{kJ/mol} \tag{5}$$

$$H_2 + \frac{1}{2}O_2 \rightarrow H_2O \qquad \Delta H^{\circ}_{298\,K} = -241.82\,\text{kJ/mol} \tag{6}$$

$$CO + \frac{1}{2}O_2 \rightarrow CO_2 \qquad \Delta H^{\circ}_{298\,K} = -282.98\,\text{kJ/mol} \tag{7}$$

Compared to regular combusting systems, in which air is fed as the fuel combusting agent, steam can influence the reaction pathway, modulate the flame temperature, and contribute to lower CO levels in the product [53].

2.3.2. Reverse Water–Gas Shift Reactor

The CO_2 produced from the OSC is fed to a reverse water gas shift catalytic reactor, where it is mixed with the hydrogen produced from the electrolyzer to ensure syngas production. The RWGS reactor requires high temperatures to retrieve CO molecules from the hydrogenation of carbon dioxide through reactions (8) to (10). The endothermic nature of the reaction (8) requires high temperatures and is thermodynamically limited, rather than kinetically. The equilibrium composition is shown in Figure 4 as a function of pressure and temperature. It is reasonably simulated as an equilibrium reactor in the following calculations for an H_2/CO_2 ratio of 3:1 at the inlet [54,55]. It can be observed that methanation is favored by thermodynamics at T < 600 °C, while above 700 °C, almost no methane is usually observed [30]. The dependence on pressure is showed by the dashed lines in Figure 4; at higher temperatures, the higher pressure enhances methane formation, but at 900 °C, hydrogen production is prevalent. Optimal conditions are found for high CO_2 conversion and an SN value close to 2 for the following methanol synthesis. Low pressures and high temperatures are preferred, as shown in Figure 4, where the SN value reaches the optimal value of 2 towards high temperatures. The SN is relevant over 600 °C, since below this value, the water–gas shift reaction is prevalent, having low production rates of hydrogen with CO_2 production, resulting in negative values of the stoichiometric ratio. High pressures can be reached and the main impact factor upon operation is methane formation [56], but the chosen pressure of 10 bar allows for lower compression of the syngas before methanol and higher compactness of the unit. The values chosen in this study are 10 bar and 900 °C to ensure high CO conversion and low selectivity towards the methanation reaction (9).

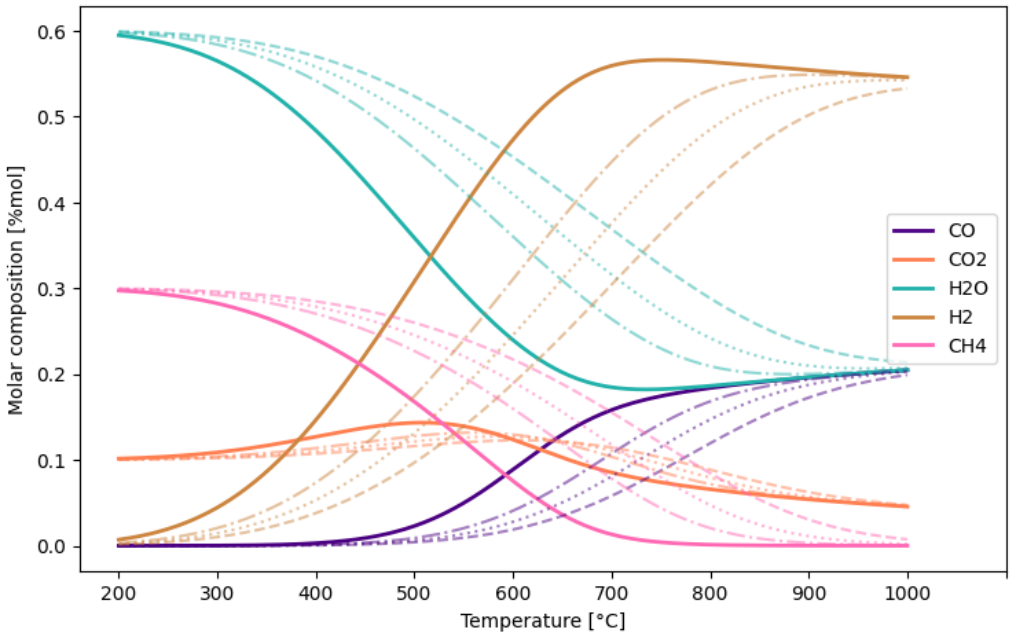

(**a**)

Figure 4. *Cont.*

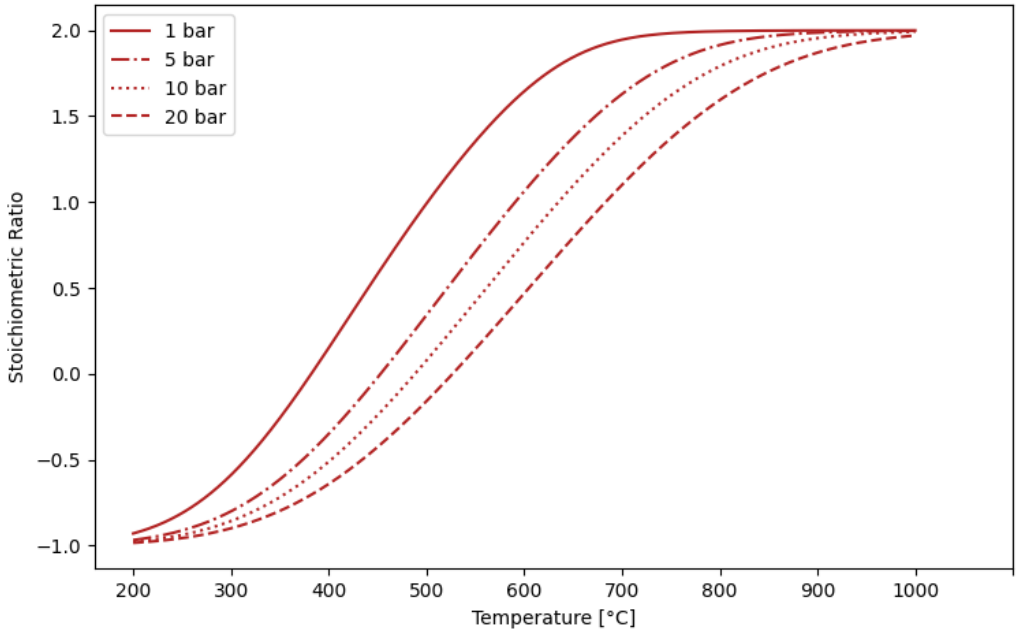

(**b**)

Figure 4. Equilibrium behavior as a function of temperature and pressure for H_2/CO_2 = 3:1 of (**a**) molar composition (**b**) syngas stoichiometric ratio (SN).

$$CO_2 + H_2 \longleftrightarrow CO + H_2O \qquad \Delta H^{\circ}_{298\,K} = +41.16\,kJ/mol \tag{8}$$

$$CO + 3H_2 \longleftrightarrow CH4 + H_2O \qquad \Delta H^{\circ}_{298\,K} = -206.5\,kJ/mol \tag{9}$$

$$CO_2 + 4H_2 \longleftrightarrow CH4 + 2H_2O \qquad \Delta H^{\circ}_{298\,K} = -165\,kJ/mol \tag{10}$$

To avoid coke deposition and catalyst deactivation, an over-stoichiometric ratio of H_2 and CO_2 was chosen. Multiple studies have been carried out with the implementation of noble and transition metals, the latter are usually picked due to the advantageous compromise between cost and activity. It is worthwhile to mention that there exists a study on RWGS carried out on $Cu/ZnO/ZrO_2/Ga_2O_3$ (5:3:1:1) catalyst [31,57].

2.3.3. Solid Oxide Electrolyzer

The solid oxide electrolyzer cell system is a fundamental unit of the process under study. This unit operates at high temperatures undergoing an electrolysis reaction upon solid fast ion-conducting oxides. The choice of a high-temperature electrolyzer is driven by the lower electrical power demand when compared to other commercial options [58]. This unit's fundamentals regard water's electrochemical decomposition to produce hydrogen and oxygen. The unit is composed of two electrodes in a basic electrolyte, connected to a direct current (DC) supply.

The reaction of decomposition of water is endothermic, once a sufficient voltage is applied to the system, the redox reactions take place (Figure 5), collecting hydrogen at the cathode and oxygen at the anode [59]. The chosen operating conditions are of 850 °C and 10 bar, to ensure higher performances [60] and allow for a lower syngas compression step before the methanol synthesis. On the anode side, an oxygen sweep was considered for a pure stream outcome [61]. The simulation of the unit in Aspen HYSYS was simplified by implying a conversion reactor and a component splitter after validation of the energy consumption from available 0D literature models [62,63].

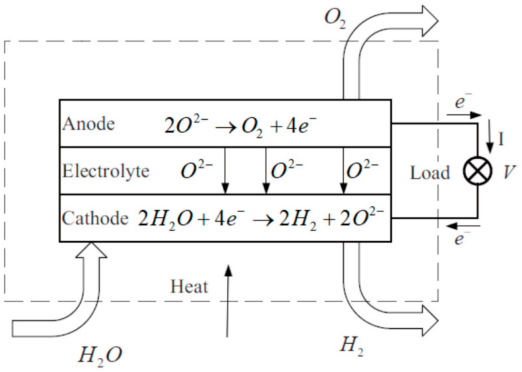

Figure 5. SOEC operation scheme, the power load is mitigated by the heat from the system that allows feeding steam to the unit [64].

2.4. Methanol Section

The methanol synthesis section follows standard commercial configurations and it is present in both Case A and Case B. The reactions are reported in (11) and (12) and the simulation was carried out as a water-cooled packed bed reactor, working at 60 bars and 250 °C filled with a $Cu/ZnO/Al_2O_3$ catalyst and a GHSV of 10,000 h^{-1} [65,66]. The chosen kinetic model is based on the one introduced by Vanden Bussche and Froment [67], reaction rates equations and relative parameters are reported in Table 2.

$$CO_2 + 3H_2 \longleftrightarrow CH_3OH + H_2O \qquad \Delta H^{\circ}_{298\,K} = -97.36\,kJ/mol \tag{11}$$

$$CO_2 + H_2 \longleftrightarrow CO + H_2O \qquad \Delta H^{\circ}_{298\,K} = +41.16\,kJ/mol \tag{12}$$

Table 2. Methanol synthesis reaction rates parameters and equations.

Expression	UoM	Equation
$r_{MeOH} = \frac{k_1 P_{CO_2} P_{H_2} \left(1 - \frac{1}{K_{eq1}} \frac{P_{H_2O} P_{MeOH}}{P_{CO_2} P_{H_2}^3}\right)}{DEN^3}$	$[\frac{mol}{kg_{cat} \cdot s}]$	(13)
$r_{WGS} = \frac{k_5 \left(P_{CO} P_{H_2O} - \frac{P_{CO_2} P_{H_2}}{K_{eq2}}\right)}{DEN}$	$[\frac{mol}{kg_{cat} \cdot s}]$	(14)
$DEN = 1 + k_2(P_{H_2O})(P_{H_2}) + k_3 {P_{H_2}}^{0.5} + k_4 P_{H_2O}$	[-]	(15)
$\log_{10} K_{eq1} = \frac{3066}{T} - 10.592$	[-]	(16)
$\log_{10} \frac{1}{K_{eq_2}} = \frac{-2073}{T} + 2.029$	[-]	(17)
$k_1 = 1.07 \exp\left(\frac{36696}{RT}\right)$	$[\frac{mol}{kg_{cat} \cdot s \cdot bar^2}]$	(18)
$k_2 = 3453.38$	[-]	(19)
$k_3 = 0.499 \exp\left(\frac{17197}{RT}\right)$	$[\frac{1}{bar^{0.5}}]$	(20)
$k_4 = 6.62 \cdot 10^{-11} \exp\left(\frac{124119}{RT}\right)$	$[\frac{1}{bar}]$	(21)
$k_5 = 1.22 \cdot 10^{10} \exp\left(\frac{-94765}{RT}\right)$	$[\frac{mol}{kg_{cat} \cdot s \cdot bar}]$	(22)

The syngas produced in the reforming section undergoes the catalytic reactor where methanol is produced. The exiting stream is sent to a condenser where the unreacted syngas is recycled to the reactor, with a 5% purge to avoid methane accumulation. The purge value chosen is based upon industrial experience, no optimization was carried out in the present work. The liquid product goes to the purification section, which is composed by two distillation columns. The first one operates at atmospheric pressure to maximize

the separation of the off-gases, while the second one operates at 4 bars, reaching 99.85 wt% purity for methanol.

2.5. Key Performance Indicator

Results were analyzed on a set of key performance indicators, to assess the overall performance of the new electrified process proposed in this work.

- Global Methanol Yield. The overall yield of the process has been defined as the amount of kg/h of methanol produced (m), over the inlet biogas to the process in kg/h (Equation (23)).

$$Y_{global,MeOH} = \frac{\dot{m}_{CH_3OH,out}}{\dot{m}_{biogas,in}} \tag{23}$$

- Conversion of Methane in the Reformer. It evaluates the amount of methane reacted in the reformer reactor, given the moles at the inlet and outlet of the process expressed in molar flowrate (kmol/h), as defined in Equation (24)

$$\chi_{CH_4} = \frac{\dot{F}_{CH_{4,in}} - \dot{F}_{CH_{4,out}}}{\dot{F}_{CH_{4,in}}} \tag{24}$$

- Methanol Reactor Yield, reported in Equation (25). The yield considers the methanol produced in the reactor over the available carbon quantity in the fresh syngas.

$$Y_{reactor,MeOH} = \frac{\dot{F}_{MeOH,reacted}}{\dot{F}_{CO,syngas} + \dot{F}_{CO_2,syngas}} \tag{25}$$

- Emitted CO_2. To appreciate the impact of the electrification upon thermal-based processes, the CO_2 directly emitted in both technologies is calculated, Equation (26). The contributions are given by CO_2 separated from the PSWA, the amount found in the flue gases (for Case A), and the synthesis off-gases.

$$E_{CO_2} = \frac{\dot{m}_{CO_2,separated} + \dot{m}_{CO_2,fluegases} + \dot{m}_{CO_2,offgas}}{\dot{m}_{CH_3OH}} \tag{26}$$

- Carbon Global Efficiency, defined in Equation (27). This parameter estimates the quantity of carbon that is exploited from the biogas available to the plant normalized on the total biogas invested in the process.

$$\eta_{C,global} = \frac{\dot{F}_{C_{CH_3OH,out}}}{\dot{F}_{C_{biogas,in}}} \tag{27}$$

- Process efficiency. As reported in (28), the ratio is between the heat content of the methanol, multiplying the mass flowrate (kg/s) of MeOH produced and its LHV (19.93 MJ/kg) and the contribution of the inlet methane content and the electricity consumption in MW.

$$\eta_{process} = \frac{\dot{m}_{C_{CH_3OH,prod}} LHV_{MeOH}}{\dot{m}_{CH_{4,biogas}} LHV_{CH_4} + Q_{electricity}} \tag{28}$$

- The Carbon Reduction Potential (CRP) is defined as (29), which gives an estimate of the carbon dioxide exploited in the process.

$$CRP = \frac{\dot{F}_{CO_2,biogas} - \dot{F}_{CO_2,outlet}}{\dot{F}_{CO_2,biogas}} \tag{29}$$

- Total Specific Energy Consumption. The electric consumption is taken into account in calculating the total electric power consumption for each case. The results are then normalized over kg of methanol produced.

3. Results and Discussion

3.1. Mass Balance

Results for the simulated cases are reported, respectively, in Tables 3 and 4. The flowrate of biogas is 500 Nm^3/h for both configurations, free from contaminants as assumed collected after necessary purification steps.

Table 3. Operating conditions and molar compositions for Case A.

Stream	**BIOG1**	**BIOG2**	**BIOG3**	**BIOG4**	**AIR**	**STEAM**	**CO2**	**MUW1**	**MUW2**
T [°C]	25	25	25	20.43	25	570	20	20	20
p [bar]	1.3	1.3	1.3	14.70	1.20	15	1	15	15
F [Nm^3/h]	500	142.50	357.50	277.60	1121	643.9	73.8	2.044	202.4
M [kg/h]	607.40	173.10	434.40	276.90	1442	517.80	143	1.643	162.64
CH_4	0.60	0.60	0.60	0.78	0	0	0	0	0
H_2O	0	0	0	0	0	1	0.01	1	1
CO_2	0.40	0.40	0.40	0.22	0	0	0.99	0	0
N_2	0	0	0	0	0.79	0	0	0	0
O_2	0	0	0	0	0.21	0	0	0	0
H_2	0	0	0	0	0	0	0	0	0
CO	0	0	0	0	0	0	0	0	0
CH_3OH	0	0	0	0	0	0	0	0	0
Stream	**SG1**	**SG2**	**FG1**	**PG1**	**PG2**	**WT1**	**WT2**	**MEOH**	
T [°C]	45	45	172	45	12.6	45	138.1	77.2	
p [bar]	14.3	60	1.01325	60	1.3	1.01325	3.5	1.5	
F [Nm^3/h]	830.5	1322	1244	69.39	9.43	368	73.55	225.8	
M [kg/h]	421.2	451.4	1588	23.92	16.39	295.9	59.26	322.5	
CH_4	0.0118	0.1303	0	0.1308	0.0766	0	0	0	
H_2O	0.071	0.009	0.1714	0.009	0.011	0.9996	0.9969	0.01	
CO_2	0.0969	0.0726	0.1429	0.0739	0.8141	0	0	0	
N_2	0	0	0.6771	0	0	0	0	0	
O_2	0	0	0.086	0	0	0	0	0	
H_2	0.6918	0.7682	0	0.7661	0.0518	0	0	0	
CO	0.1924	0.0226	0	0.0228	0.0843	0	0	0	
CH_3OH	0	0	0	0.054	0.0479	0	0	0.99	

In Case A, almost 30% of the feedstock has to be invested as fuel in the furnace while the remaining part undergoes partial removal of CO_2, finding an optimal composition of 78% of CH_4 and 22% of carbon dioxide before the reforming reactor. These conditions strongly depend on the water circulated in the PSWA, which at 15 bar, results in 322 lt/h pumped for a total removal of 143 kg/h of CO_2. The carbon dioxide treatment for possible commercialization is not considered in the study, but the stream is assumed to be either implemented within other processes or stocked. Air is compressed by a blower and fed in excess to stoichiometric conditions; it is mixed with fuel and preheated before entering the furnace. Flue gases from the furnace are cooled below 200 °C with 8 mol% oxygen content, after heat recovery in the convective zone of the furnace. On the reactive side of the reformer, the SC ratio is close to 3 and the syngas produced has a tenor of hydrogen of 69.18 mol%. The configuration allows for a yearly methanol production of 2.7 ktons.

The second configuration results are reported in Table 4 (Case B) allows using the integrity of biogas in the OSC unit, with a full conversion of the methane fraction to CO_2 and water. After condensation, the stream is sent to a compressor to reach the selected pressure of 10 bar, as required by the RWGS. To reach the syngas SN value of 2 at the outlet

of the RWGS, 156.8 kg/h of hydrogen are necessary from the SOEC at 10 bar. Along with hydrogen production, the electrolyzer provides a stream of oxygen, of which almost 82% is employed in the OSC chamber, while 207.7 kg/h can be stocked and sold as a product or implied within close process facilities. The syngas produced in the RWGS, SG1, is sent to the methanol synthesis. The product stream undergoes purification, producing almost 6 ktons per year of methanol. This process requires three condensation steps for water separation which, after undergoing degassing and being integrated by a make-up stream, is used as a source for the steam demanded by the OSC and SOEC.

Table 4. Operating conditions and molar compositions for Case B.

Stream	**BIOG1**	**CO2**	**HY1**	**OX1**	**OX2**	**STEAM1**	**STEAM2**	**MUW0**
T [°C]	25	600	600	120	120	25	25	25
p [bar]	1.01	10	10	10	10	1.01	1.01	1.01
F [Nm^3/h]	500	591.70	1616	797.80	652.30	2609.0	2134.0	401.9
M [kg/h]	607.4	1083.0	156.8	1139.0	931.3	2087.0	1715.0	323.0
CH_4	0.60	0	0	0	0	0	0	0
H_2O	0	0.11	0.01	0	0	1	1	1
CO_2	0.40	0.89	0	1	1	0	0	0
N_2	0	0	0	0	0	0	0	0
O_2	0	0	0	0	0	0	0	0
H_2	0	0	0.99	0	0	0	0	0
CO	0	0	0	0	0	0	0	0
CH_3OH	0	0	0	0	0	0	0	0
Stream	**SG1**	**SG2**	**PG1**	**PG2**	**WT1**	**WT2**	**MEOH**	
T [°C]	321.2	45	45	13	45	137.7	77.2	
p [bar]	61	60	60	1.30	1.30	3.50	1.50	
F [Nm^3/h]	1753.0	2504.0	131.80	19.48	455.4	114.0	495.1	
M [kg/h]	873.2	738.9	38.89	34.98	366.1	91.96	707.2	
CH_4	0	0	0	0	0	0	0	
H_2O	0.01	0	0	0	0.99	0.99	0.01	
CO_2	0.08	0.07	0.07	0.85	0.01	0	0	
N_2	0	0	0	0	0	0	0	
O_2	0	0	0	0	0	0	0	
H_2	0.68	0.90	0.90	0.09	0	0	0	
CO	0.23	0.03	0.03	0.01	0	0	0	
CH_3OH	0	0	0	0.05	0	0.01	0.99	

3.2. Energy Balance

The overall electric consumptions are reported in Table 5 for the two simulated configurations. The standard industrial technology, due to the thermal nature of the process, can sustain the endothermic reforming reaction through the heat released in the furnace. For Case B, the RWGS endothermic reaction is sustained by the OSC unit, but the necessary oxygen to meet total combustion of the fuels, and the hydrogen to reach the required SN value, is provided by the electricity provided to the SOEC. The main source of consumption in Case B is given by the electrolyzer, which counts for 95% of the overall consumption. As expected, in Case B the syngas compressors require higher consumption due to the higher flowrates of gas treated. For better comprehension of the energy integration systems, thermal loads across the processes were analyzed with the Aspen Energy Analyzer. As reported in Figure 6, both systems show a demand for cooling utilities. The hot zone of the processes can sustain steam generation, with additional heat to spare, for example, to be recovered for the anaerobic digestor heating. The total cooling utility demand for Case A is of 0.58 MW of cooling, while in Case B 3.7 MW. The big difference is associated with the different condensation steps required, the first case requires the condensation of water after the SMR only, while the second one, must remove water after the OSC, the RWGS, and

SOEC. In Table 6 it can be observed the different demand of cooling content for the two cases. The hot region available for Case B is due to the high operating temperatures of the three main reacting units of the systems. Due to the absence of nitrogen, the OSC allows for high temperatures in the combustion chamber, as in common combustion systems. The necessity to condense water before entering the RWGS, operating at 850 °C, introduces a high-temperature jump, which allows recovering heat for steam, but with a strong demand on cooling utility. The choice of a high-temperature electrolyzer has been taken due to the nature of the process, a SOEC allows to lower the electricity demand by recovering more heat in the steam fed to the unit.

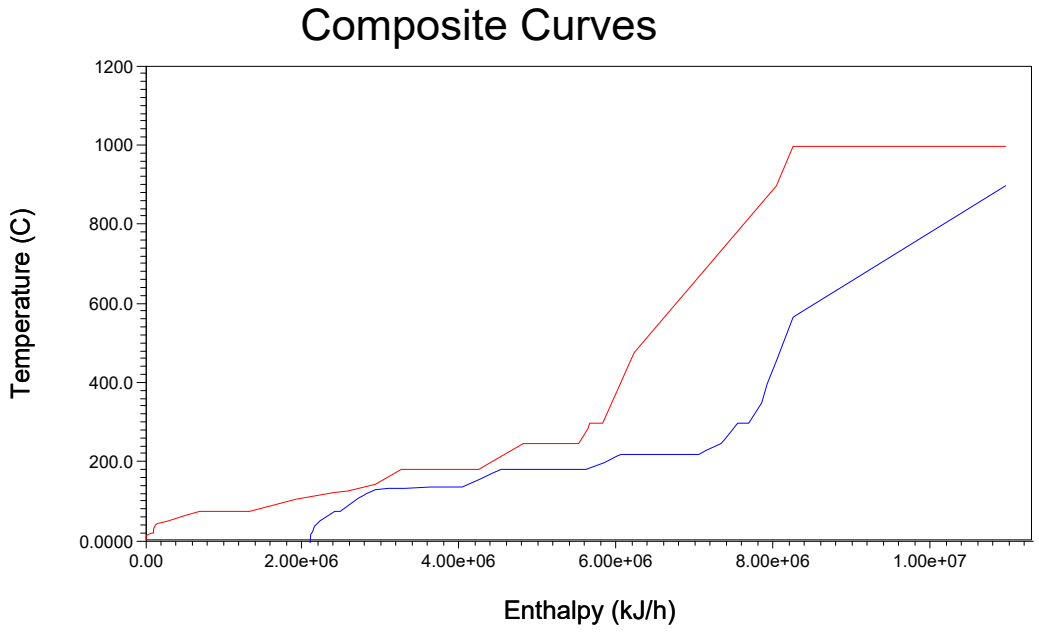

(**a**)

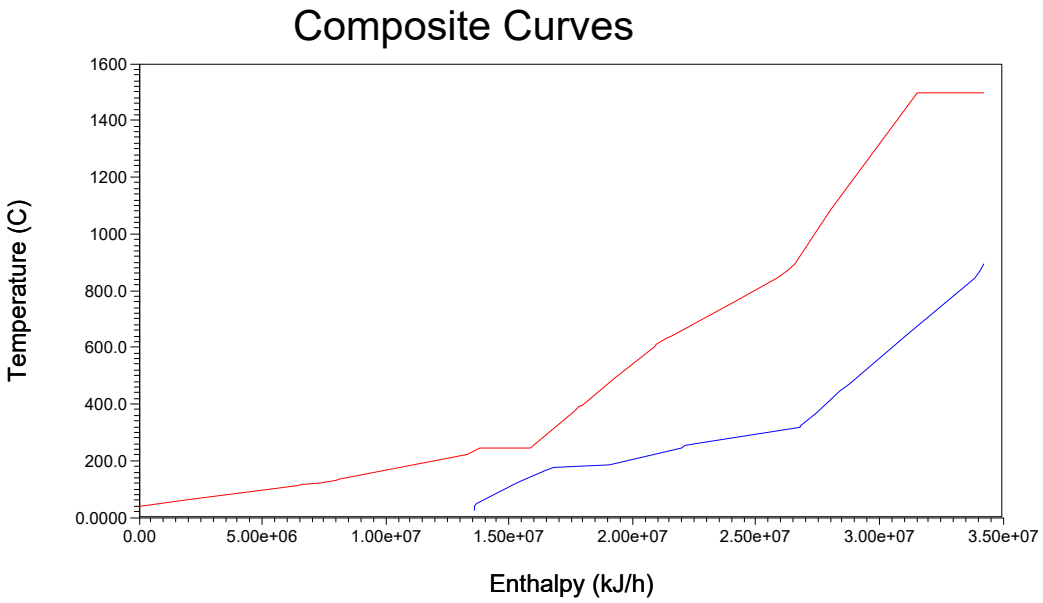

(**b**)

Figure 6. Thermal loads for hot (red line) and cold (blue line) (**a**) Case A and (**b**) Case B obtained from Aspen Energy Analyzer tool.

Table 5. Equipment power consumption for Case A and Case B.

Equipment	Unit	Case A	Case B
Biogas compressor	kW	44	-
Water recycle pump	kW	16.22	-
Air blower	kW	-	-
SOEC	kW	-	5260.68
Water pump	kW	-	2.458
CO_2 compressor	kW	-	81.76
Syngas compressor	kW	65.79	182.5
Unconverted syngas recycle compressor	kW	4.139	8.23
Total Consumption	kW	130.15	5535.63

Table 6. Energy integration results for Case A and Case B.

	UoM	Case A	Case B
Total heating demand	MW	0	0
Total cooling demand	MW	0.58	3.7

3.3. Key Performance Indicators

The key performance indicators are summarized in Table 7 for the four cases under study. Results are normalized to provide a proper comparison, given that the studies found in the literature operated on different biogas-size plants. Case A and Case C are directly compared to evaluate the uncommon smaller-scale plant results. The two process configurations differ only in the CO_2 separation method, the one considered for this study opted for a partial upgrading through water absorption, rather than total separation with amine, as in Case C. Case D has been included to better understand results from Case B, especially in energetic consumption terms. Both scenarios provide electrification of the RWGS reactor, Case B supports the endothermicity of the reactor with the OSC, while Case D directly employs electrical energy. Also in this comparison, the similarities between the results are noticeable.

The two opposing technologies differ strongly in methanol global yield; this directly depends on the necessity of the SMR processes to invest some of the feedstock as fuel, while in the electrified process (Case B), the integrity of the feedstock is interested in the reaction and the CO_2-rich stream is integrated with H_2 to produce valuable syngas. Furthermore, methane conversion is total in Case B since the OSC consumes it integrally through the oxygen from the SOEC. Methanol reactor yield strongly depends on the operating conditions of the synthesis, in particular, the SN ratio highly impacts it.

This study's results are similar (Case A 93.76% 0 Case B 93.80%) due to the boundary conditions of an SN value equal to 2.05 at the inlet of the methanol reactor. Carbon dioxide directly emitted, in Case B, is below unity while in Case A SMR is heated by the combustion of biogas and carbon dioxide-rich flue gas is introduced into the atmosphere. Sources of carbon differ strongly in the two cases, Case B has only one voice of emission, which is the carbon dioxide content in the synthesis purge gas, while Case A has both the CO_2 separated by the PSWA and the content in the flue gas.

Global carbon efficiency is quite lower for SMR processes due to the amount of carbon used in the combustion rather than its availability to the synthesis, Case D has lower values since it invests biogas in biomethane production and only the remaining carbon dioxide in the methanol synthesis. Some further considerations have been carried out to visualize the carbon intensity of the process better. Reported in Figure 7 is the relationship between the carbon intensity and the amount of CO_2 emitted in the methanol production. If electrical energy had no emission intensity, this process would be entirely carbon negative, since the CO_2 emitted compared to the amount fed, over kg of MeOH produced, is around -507 $gCO_2/kgMeOH$. Carbon neutrality is met at 75 gCO_2/kWh; therefore, the impact of the system strongly depends on the carbon intensity of the country and energy source.

In Europe, France and Sweden have a low impact due to nuclear and renewable power. In these countries, Case B would have a competitively low GHG impact, while in Italy, for example, the system would highly benefit from the introduction of renewable electricity sources. This suggests the necessity of combining electrified industrial processes with renewables.

Table 7. Key performance indicators of the SMR, the outer electrified process, previous results from Rinaldi et al. [35] and Basini et al. [40]

Key Parameter	UoM	Case A	Case B	Case C	Case D
$Y_{global,MeOH}$	kg_{MeOH}/kg_{Biogas}	0.58	1.16	0.61	0.41
χ_{CH_4}	%	94.90	100	95.31	-
$Y_{reactor,MeOH}$	%	93.76	93.80	99.42	-
E_{CO_2}	$kg_{CO_2}/kgCH_3OH$	1.38	0.008	1.23	0.15
$\eta_{C,global}$	%	33.45	66.32	34.74	15.34
$\eta_{process}$	%	63.2	49.38	64.32	23.85
CRP	%	−25.61	91.42	−15.71	90.27
Total Electric Power Consump.	kWh/kg_{MeOH}	0.4	6.98	0.55	11.36

The process efficiency is a relevant indicator of the system's energy efficiency. The electrified processes require a large amount of electric energy, SMR ones show an efficiency of 63–64% exploiting methane calorific value. It is interesting to notice how Case B presents 49% efficiency compared to Case D's 24% efficiency. The introduction of the OSC allows for a lower energy demand from the electrolyzer, consequently, a higher energetical efficiency is recovered.

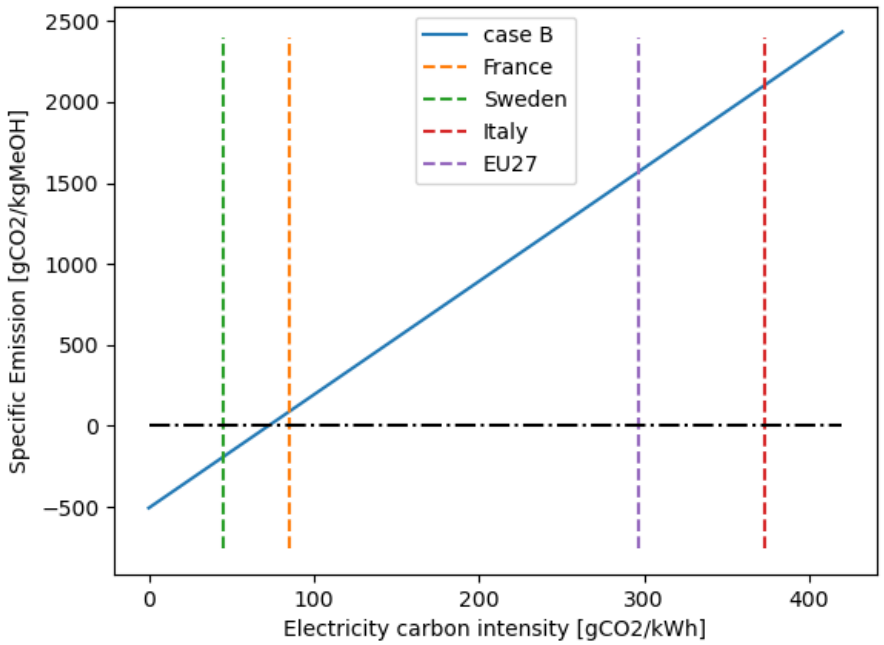

Figure 7. Specific CO_2 emission in the MeOH production, against the emission intensity factor. Reference values are 85 for France, 45 for Sweden, 373 for Italy, and 297 for the European Union, measured in gCO_2/kWh [68].

The total carbon potential underlines the biggest advantage in the electrified processes, the amount of captured CO_2 is in the order of 90% for the global balance. SMR technologies present a negative value due to the upgrading step of biogas, the amount of carbon dioxide removed strongly impacts on the total direct emissions, as well as the exhaust percentage derived by burning off-gases in the system.

Lastly, the energy consumption is given; for the SMR technologies, the main contribution is given by the gas compressors, 0.35 kWh/kg of MeOH for Case A and 0.49 kWh/kg of MeOH for Case C, while for the electrified processes, the electrolyzer is the major source. Case B, using a SOEC working at high temperatures, consumes 6.6 kWh/kg of MeOH, and Case D, exploiting a PEM electrolyzer at lower temperatures, 10.6 kWh/kg of MeOH. This result favors the use of a high-temperature electrolyzer for a lower energy consumption if the system has available heat.

4. Conclusions

The current work provides interesting results upon integrating an innovative reforming process. The autothermal outer electrification introduces an OSC chamber that allows heat recovery from the burning in oxy-steam conditions of the fraction of methane at the biogas inlet. Results from a 1 MW biogas plant application have shown the lowest impact of an electrified process (0.008 $kgCO_2$/kgMeOH emitted) compared to conventional thermal SMR (1.38 $kgCO_2$/kgMeOH emitted). Productivity-wise, CCU technologies exploit carbon dioxide as a reactant rather than an emission; the process of interest (Case B) shows a 1.16 kgMeOH/kgbiogas production, since the integrity of the feedstock is spent in the synthesis, rather than the 28% spent as fuel in SMR (Case A). The introduction of a high-temperature electrolyzer SOEC accounts for 94% of the energy demand, bringing to a total of 7 kWh/kgMeOH produced. A comparison with a literature study on an electrified RWGS shows how OSC allows for an overall lower energy demand, as well as a higher sequestration rate in MeOH production (66.32% global carbon efficiency from the total amount of biogas available). Negative carbon impact can be reached below 75 gCO_2/kWh electricity intensity, a condition that can be met by exploiting renewable electricity sources. Overall, the technology shows good potential in biogas to fuel applications, the main drawback lays within the cooling utility demand, which is quite high. Further studies will focus on rigorous economic and environmental assessments to additionally validate these preliminary results, compared with alternative electrification, as well.

5. Patents

Manenti F., Bisotti F., Politecnico di Milano Patent Number: PCT/EP2023/060525, 2022.

Supplementary Materials: The following supporting information can be downloaded at: https://www.mdpi.com/article/10.3390/pr12081598/s1.

Author Contributions: Conceptualization, L.S.; Methodology, L.S., G.B. and F.M.; Validation, L.S., M.M.B. and S.C.; Formal analysis, L.S.; Investigation, L.S.; Data curation, M.M.B. and S.C.; Writing—original draft, L.S. and G.B.; Writing—review & editing, L.S. and G.B.; Supervision, G.B. and F.M.; Project administration, F.M. All authors have read and agreed to the published version of the manuscript.

Funding: This research received no external funding.

Data Availability Statement: Data are contained within the article and the provided Supplementary Materials.

Conflicts of Interest: The authors declare no conflicts of interest.

Abbreviations

The following abbreviations are used in this manuscript:

BFW	Boiling Feed Water
CAGR	Compound Annual Growth Rate
CBM	Compressed BioMethane
CCS	Carbon Capture and Storage
CCU	Carbon Capture and Utilization

DME	Dymethylether
GHG	Greenhouse Gases
GHSV	Gas Hourly Space Velocity
LHV	Lower Heating Value
LBM	Liquefied BioMethane
MeOH	Methanol
OSC	Oxy-Steam Combustion
PSA	Pressure Swing Absorption
PSWA	Pressure Swing Water Absoprtion
PTX	Power to X
RWGS	Reverse Water–Gas Shift
SC	Steam=to-Carbon ratio
SMR	Steam Methane Reformer
SOEC	Solid Oxide Electrolysis Cell
UoM	Unit of Measure

References

1. *World Energy Outlook 2023*; Technical Report; IEA: Paris, France, 2023.
2. Song, H.; Liu, Y.; Bian, H.; Shen, M.; Lin, X. Energy, environment, and economic analyses on a novel hydrogen production method by electrified steam methane reforming with renewable energy accommodation. *Energy Convers. Manag.* **2022**, *258*, 115513 . [CrossRef]
3. Commission, E. 2050 Long Term Strategy. 2024. Available online: https://climate.ec.europa.eu/eu-action/climate-strategies-targets/2050-long-term-strategy_en (accessed on 16 April 2024).
4. Commission, E. REPowerEU: Energy Policy in EU Countries' Recovery and Resilience Plans. 2024. Available online: https://www.consilium.europa.eu/en/policies/eu-recovery-plan/repowereu/ (accessed on 7 June 2024).
5. Mion, A.; Galli, F.; Mocellin, P.; Guffanti, S.; Pauletto, G. Electrified methane reforming decarbonises methanol synthesis. *J. CO_2 Util.* **2022**, *58*, 101911. [CrossRef]
6. Nawaz, A.; Razzak, S.A. Co-pyrolysis of biomass and different plastic waste to reduce hazardous waste and subsequent production of energy products: A review on advancement, synergies, and future prospects. *Renew. Energy* **2024**, *224*, 120103. [CrossRef]
7. Liebetrau, J.; Ammenberg, J.; Gustafsson, M.; Pelkmans, L.; Murphy, J.D. The role of biogas and biomethane in pathway to net zero. In *IEA Bioenergy Task 37*; IEA Bioenergy: Florence, Italy, 2022.
8. EBA Statistical Report 2023. 2023. Available online: https://www.europeanbiogas.eu/eba-statistical-report-2023/ (accessed on 16 April 2024).
9. Stato Dell'arte Biogas in Italia. Available online: https://www.venetoagricoltura.org/wp-content/uploads/2020/10/Banzato.pdf (accessed on 16 April 2024).
10. Della Repubblica Italiana, G.U. Decreto Ministeriale. Available online: https://www.gazzettaufficiale.it/ (accessed on 16 April 2024).
11. Benato, A.; Macor, A. Italian biogas plants: Trend, subsidies, cost, biogas composition and engine emissions. *Energies* **2019**, *12*, 979. [CrossRef]
12. Kaparaju, P.; Rintala, J. 17-Generation of heat and power from biogas for stationary applications: Boilers, gas engines and turbines, combined heat and power (CHP) plants and fuel cells. In *The Biogas Handbook*; Wellinger, A., Murphy, J., Baxter, D., Eds.; Woodhead Publishing Series in Energy; Woodhead Publishing: Sawston, UK, 2013; pp. 404–427. [CrossRef]
13. Yang, L.; Ge, X. Biogas and Syngas Upgrading. In *Advances in Bioenergy*; Elsevier Inc.: Amsterdam, The Netherlands, 2016; Volume 1, pp. 125–188. [CrossRef]
14. Sun, Z.F.; Zhao, L.; Wu, K.K.; Wang, Z.H.; Wu, J.t.; Chen, C.; Yang, S.S.; Wang, A.J.; Ren, N.Q. Overview of recent progress in exogenous hydrogen supply biogas upgrading and future perspective. *Sci. Total Environ.* **2022**, *848*, 157824. [CrossRef]
15. Marchese, M.; Giglio, E.; Santarelli, M.; Lanzini, A. Energy performance of Power-to-Liquid applications integrating biogas upgrading, reverse water gas shift, solid oxide electrolysis and Fischer-Tropsch technologies. *Energy Convers. Manag. X* **2020**, *6*, 100041. [CrossRef]
16. Kumar, R.; Kumar, A.; Pal, A. Overview of hydrogen production from biogas reforming: Technological advancement. *Int. J. Hydrog. Energy* **2022**, *47*, 34831–34855. [CrossRef]
17. Zhao, X.; Joseph, B.; Kuhn, J.; Ozcan, S. Biogas Reforming to Syngas: A Review. *iScience* **2020**, *23*, 101082. [CrossRef] [PubMed]
18. Abdin, Z.; Zafaranloo, A.; Rafiee, A.; Mérida, W.; Lipiński, W.; Khalilpour, K.R. Hydrogen as an energy vector. *Renew. Sustain. Energy Rev.* **2020**, *120*, 109620. [CrossRef]
19. Lee, B.; Heo, J.; Kim, S.; Sung, C.; Moon, C.; Moon, S.; Lim, H. Economic feasibility studies of high pressure PEM water electrolysis for distributed H_2 refueling stations. *Energy Convers. Manag.* **2018**, *162*, 139–144. [CrossRef]
20. Navas-Anguita, Z.; García-Gusano, D.; Dufour, J.; Iribarren, D. Revisiting the role of steam methane reforming with CO_2 capture and storage for long-term hydrogen production. *Sci. Total Environ.* **2021**, *771*, 145432. [CrossRef] [PubMed]

21. Simpson, A.P.; Lutz, A.E. Exergy analysis of hydrogen production via steam methane reforming. *Int. J. Hydrogen Energy* **2007**, *32*, 4811–4820. [CrossRef]
22. Do, T.N.; Kwon, H.; Park, M.; Kim, C.; Kim, Y.T.; Kim, J. Carbon-neutral hydrogen production from natural gas via electrified steam reforming: Techno-economic-environmental perspective. *Energy Convers. Manag.* **2023**, *279*, 116758. [CrossRef]
23. Maporti, D.; Nardi, R.; Guffanti, S.; Vianello, C.; Mocellin, P.; Pauletto, G. Techno-economic Analysis of Electrified Biogas Reforming. *Chem. Eng. Trans.* **2022**, *96*, 163–168. [CrossRef]
24. From, T.N.; Partoon, B.; Rautenbach, M.; Østberg, M.; Bentien, A.; Aasberg-Petersen, K.; Mortensen, P.M. Electrified steam methane reforming of biogas for sustainable syngas manufacturing and next-generation of plant design: A pilot plant study. *Chem. Eng. J.* **2024**, *479*, 147205. [CrossRef]
25. Onthong, U.; Juntarachat, N. Evaluation of biogas production potential from raw and processed agricultural wastes. *Energy Procedia* **2017**, *138*, 205–210. [CrossRef]
26. Demirbas, A. Biogas production from the organic fraction of municipal solid waste. *Energy Sources Recovery Util. Environ. Eff.* **2006**, *28*, 1127–1134. [CrossRef]
27. Calbry-Muzyka, A.; Madi, H.; Rüsch-Pfund, F.; Gandiglio, M.; Biollaz, S. Biogas composition from agricultural sources and organic fraction of municipal solid waste. *Renew. Energy* **2022**, *181*, 1000–1007. [CrossRef]
28. Lackey, J.C.; Peppley, B.; Champagne, P.; Maier, A. Composition and uses of anaerobic digestion derived biogas from wastewater treatment facilities in North America. *Waste Manag. Res.* **2015**, *33*, 767–771. [CrossRef]
29. Ostadi, M.; Paso, K.G.; Rodriguez-Fabia, S.; Øi, L.E.; Manenti, F.; Hillestad, M. Process Integration of Green Hydrogen: Decarbonization of Chemical Industries. *Energies* **2020**, *13*, 4859. [CrossRef]
30. González-Castaño, M.; Dorneanu, B.; Arellano-García, H. The reverse water gas shift reaction: A process systems engineering perspective. *React. Chem. Eng.* **2021**, *6*, 954–976. [CrossRef]
31. Joo, O.S.; Jung, K.D.; Moon, I.; Rozovskii, A.Y.; Lin, G.I.; Han, S.H.; Uhm, S.J. Carbon Dioxide Hydrogenation To Form Methanol via a Reverse-Water-Gas-Shift Reaction (the CAMERE Process). *Ind. Eng. Chem. Res.* **1999**, *38*, 1808–1812. [CrossRef]
32. Rezaei, E.; Dzuryk, S. Techno-economic comparison of reverse water gas shift reaction to steam and dry methane reforming reactions for syngas production. *Chem. Eng. Res. Des.* **2019**, *144*, 354–369. [CrossRef]
33. Ghosh, S.; Uday, V.; Giri, A.; Srinivas, S. Biogas to methanol: A comparison of conversion processes involving direct carbon dioxide hydrogenation and via reverse water gas shift reaction. *J. Clean. Prod.* **2019**, *217*, 615–626. [CrossRef]
34. dos Santos, R.O.; Santos, L.d.S.; Prata, D.M. Simulation and optimization of a methanol synthesis process from different biogas sources. *J. Clean. Prod.* **2018**, *186*, 821–830. [CrossRef]
35. Rinaldi, R.; Lombardelli, G.; Gatti, M.; Visconti, C.G.; Romano, M.C. Techno-economic analysis of a biogas-to-methanol process: Study of different process configurations and conditions. *J. Clean. Prod.* **2023**, *393*, 136259. [CrossRef]
36. Previtali, D.; Vita, A.; Bassani, A.; Italiano, C.; Amaral, A.F.; Pirola, C.; Pino, L.; Palella, A.; Manenti, F. Methanol synthesis: A distributed production concept based on biogas plants. *Chem. Eng. Trans.* **2018**, *65*, 409–414. [CrossRef]
37. Zhu, L.; Wang, Y.; Wang, Y.; Wang, Z. The design of new process, parametric analysis, technical and economic analysis of methanol production from biogas. *Multiscale Multidiscip. Model. Exp. Des.* **2022**, *5*, 351–364. [CrossRef]
38. Bobadilla, L.F.; Azancot, L.; González-Castaño, M.; Ruíz-López, E.; Pastor-Pérez, L.; Durán-Olivencia, F.J.; Ye, R.; Chong, K.; Blanco-Sánchez, P.H.; Wu, Z.; et al. Biomass gasification, catalytic technologies and energy integration for production of circular methanol: New horizons for industry decarbonisation. *J. Environ. Sci.* **2024**, *140*, 306–318. [CrossRef]
39. Advisors, M. Global Biomethanol Market Research Report: Forecast (2024–2030). Available online: https://www.marknteladvisors.com/research-library/biomethanol-market.html (accessed on 10 June 2024).
40. Basini, L.; Furesi, F.; Baumgärtl, M.; Mondelli, N.; Pauletto, G. CO_2 capture and utilization (CCU) by integrating water electrolysis, electrified reverse water gas shift (E-RWGS) and methanol synthesis. *J. Clean. Prod.* **2022**, *377*, 134280. [CrossRef]
41. Bozzano, G.; Pirola, C.; Italiano, C.; Pelosato, R.; Vita, A.; Manenti, F. Biogas: A Possible New Pathway to Methanol? *Comput. Aided Chem. Eng.* **2017**, *40*, 523–528. [CrossRef]
42. Hernández, B.; Martín, M. Optimal Process Operation for Biogas Reforming to Methanol: Effects of Dry Reforming and Biogas Composition. *Ind. Eng. Chem. Res.* **2016**, *55*, 6677–6685. [CrossRef]
43. Fiedler, E.; Grossmann, G.; Kersebohm, D.B.; Weiss, G.; Witte, C. *Ullmann's Encyclopedia of Industrial Chemistry*; Wiley: Hoboken, NJ, USA, 2005.
44. Rostrup-Nielsen, J.R. New aspects of syngas production and use. *Catal. Today* **2000**, *63*, 159–164. [CrossRef]
45. Bauer, F.; Persson, T.; Hulteberg, C.; Tamm, D. Biogas upgrading–technology overview, comparison and perspectives for the future. *Biofuel. Bioprod. Biorefin.* **2013**, *7*, 499–511. [CrossRef]
46. Struk, M.; Kushkevych, I.; Vítězová, M. Biogas upgrading methods: recent advancements and emerging technologies. *Rev. Environ. Sci. Biotechnol.* **2020**, *19*, 651–671. [CrossRef]
47. Sun, Q.; Li, H.; Yan, J.; Liu, L.; Yu, Z.; Yu, X. Selection of appropriate biogas upgrading technology—A review of biogas cleaning, upgrading and utilisation. *Renew. Sustain. Energy Rev.* **2015**, *51*, 521–532. [CrossRef]
48. Chen, X.Y.; Vinh-Thang, H.; Ramirez, A.A.; Rodrigue, D.; Kaliaguine, S. Membrane gas separation technologies for biogas upgrading. *RSC Adv.* **2015**, *5*, 24399–24448. [CrossRef]
49. Santos, R.; Prifti, K.; Prata, D.; Secchi, A.; Manenti, F. Techno-economic Analysis of the Syngas Conditioning from Biogas Using PSA and Pswa: Case Study of Methanol Synthesis. *Chem. Eng. Trans.* **2023**, *99*, 673–678. [CrossRef]

50. Xu, J.; Froment, G.F. Methane steam reforming: II. Diffusional limitations and reactor simulation. *AIChE J.* **1989**, *35*, 97–103. [CrossRef]
51. Tacchino, V.; Costamagna, P.; Rosellini, S.; Mantelli, V.; Servida, A. Multi-scale model of a top-fired steam methane reforming reactor and validation with industrial experimental data. *Chem. Eng. J.* **2022**, *428*, 131492. [CrossRef]
52. Department of Energy. *Improving Process Heating System Performance*; Department of Energy: Washington, DC, USA, 2015.
53. Zou, C.; Song, Y.; Li, G.; Cao, S.; He, Y.; Zheng, C. The chemical mechanism of steam's effect on the temperature in methane oxy-steam combustion. *Int. J. Heat Mass Transf.* **2014**, *75*, 12–18. [CrossRef]
54. Kirsch, H.; Sommer, U.; Pfeifer, P.; Dittmeyer, R. Power-to-fuel conversion based on reverse water-gas-shift, Fischer-Tropsch Synthesis and Hydrocracking: Mathematical modeling and simulation in Matlab/Simulink. *Chem. Eng. Sci.* **2020**, *227*, 115930. [CrossRef]
55. Callaghan, C.A.; Burke, A.A. *Kinetics and Catalysis of the Water-Gas-Shift Reaction: A Microkinetic and Graph Theoretic Approach*; Technical Report; University of Utah: Salt Lake City, UT, USA, 2006.
56. Adelung, S.; Maier, S.; Dietrich, R.U. Impact of the reverse water-gas shift operating conditions on the Power-to-Liquid process efficiency. *Sustain. Energy Technol. Assess.* **2021**, *43*, 100897. [CrossRef]
57. Ince, M.C.; Koybasi, H.H.; Avci, A.K. Modeling of reverse water–gas shift reaction in a membrane integrated microreactor. *Catal. Today* **2023**, *418*, 114130. [CrossRef]
58. Hillestad, M.; Ostadi, M.; Alamo Serrano, G.D.; Rytter, E.; Austbø, B.; Pharoah, J.G.; Burheim, O.S. Improving carbon efficiency and profitability of the biomass to liquid process with hydrogen from renewable power. *Fuel* **2018**, *234*, 1431–1451. [CrossRef]
59. Smolinka, T.; Ojong, E.T.; Garche, J. Hydrogen Production from Renewable Energies-Electrolyzer Technologies. In *Electrochemical Energy Storage for Renewable Sources and Grid Balancing*; Elsevier Inc.: Amsterdam, The Netherlands, 2015; pp. 103–128. [CrossRef]
60. Rizvandi, O.B.; Frandsen, H.L. Modeling of single- and double-sided high-pressure operation of solid oxide electrolysis stacks. *Int. J. Hydrogen Energy* **2023**, *48*, 30102–30119. [CrossRef]
61. Subotić, V.; Futamura, S.; Harrington, G.F.; Matsuda, J.; Natsukoshi, K.; Sasaki, K. Towards understanding of oxygen electrode processes during solid oxide electrolysis operation to improve simultaneous fuel and oxygen generation. *J. Power Sources* **2021**, *492*, 229600. [CrossRef]
62. Zhao, Y.; Xue, H.; Jin, X.; Xiong, B.; Liu, R.; Peng, Y.; Jiang, L.; Tian, G. System level heat integration and efficiency analysis of hydrogen production process based on solid oxide electrolysis cells. *Int. J. Hydrogen Energy* **2021**, *46*, 38163–38174. [CrossRef]
63. Menon, V.; Janardhanan, V.M.; Deutschmann, O. A mathematical model to analyze solid oxide electrolyzer cells (SOECs) for hydrogen production. *Chem. Eng. Sci.* **2014**, *110*, 83–93. [CrossRef]
64. Hou, D.; Ma, W.; Hu, L.; Huang, Y.; Yu, Y.; Wan, X.; Wu, X.; Li, X. Modeling of Nonlinear SOEC Parameter System Based on Data-Driven Method. *Atmosphere* **2023**, *14*, 1432. [CrossRef]
65. Bozzano, G.; Manenti, F. Efficient methanol synthesis: Perspectives, technologies and optimization strategies. *Prog. Energy Combust. Sci.* **2016**, *56*, 71–105. [CrossRef]
66. Cui, X.; Kær, S.K. A comparative study on three reactor types for methanol synthesis from syngas and CO_2. *Chem. Eng. J.* **2020**, *393*, 124632. [CrossRef]
67. Bussche, K.; Froment, G. A Steady-State Kinetic Model for Methanol Synthesis and the Water Gas Shift Reaction on a Commercial $Cu/ZnO/Al_2O_3$ Catalyst. *J. Catal.* **1996**, *161*, 1–10. [CrossRef]
68. Carbon Intensity Electricity. Available online: https://ourworldindata.org/grapher/carbon-intensity-electricity (accessed on 30 April 2024).